

The Analytical Theory of Bulk Melting II: Variational Method Solution in the FCC Crystal

Yajun Zhou y and Xiaofeng Jin z

Surface Physics Laboratory & Department of Physics, Fudan University, Shanghai 200433, China
(Dated: February 8, 2020)

Continuing the arguments in Paper I (arXiv: cond-mat/0405487), we model the evolution of interstitialcies with respect to temperature in a surface-free face-centered-cubic (fcc) crystal and obtain the free energy and correlation behavior based on variational methods. We show that the avalanche of interstitialcies is the instability mechanism at the melting point that bridges Lindemann criterion and Born criterion together in three dimensions.

PACS numbers: 64.70.Dv, 64.60.Qb

I. INTRODUCTION

Bulk melting is a solid-liquid phase transition taking place in a surface-free crystal.¹ It helps to clarify the essential driving force of the inhomogeneous transition out of a homogeneous system in that the surface-free condition rules out the influence of inhomogeneity at the boundary. Many attempts have been made to test the previous melting theories by studying the behavior of bulk melting,² especially in search of the relation between the widely-cited Lindemann³ and Born⁴ criteria.

In the recent molecular dynamics simulation contributed by Jin et al.,⁵ it is demonstrated that the melting point of a surface-free Ar crystal does satisfy both Lindemann and Born criteria. In Ref.⁵, the Ar crystal melts when the shear modulus see a sudden downfall (albeit not vanishing, which is consistent with the experimental measurements⁶) and the atom displacement surges to infinity simultaneously. Jin et al. have attributed this coincidence to the "Lindemann particle" (atom with displacement larger than ℓ times the atom spacing) clusters that emerge sporadically at low temperatures but abound throughout the crystal when melting point is approached. It is found that within such energetic atom clusters, the shear modulus $(C_{11}^B - C_{12}^B)/2$ is almost zero. Judging the role of Lindemann particle clusters that satisfy both the Born and Lindemann instability criteria, it is then concluded in Ref.⁵ that melting is governed by the "strongly-correlated" Lindemann and Born perspectives. However, it is still too early to declare the final reconciliation between the two criteria before one is convinced that the results in Ref.⁵ have some general validity in the context of the underlying physical pathway towards melting that links the Lindemann and Born scenarios.

In this paper, we extend the discussions in Paper I to the 3D fcc crystal. Following the idea of defect-motivated transition in previous literature^{8,9,10,11} and the previous understandings of defect cooperation^{9,12,13,14,15,16,17,18,19}, we use the J_1 - J_2 model plus vibrational Hamiltonian²⁰ to formulate the cooperative creation and the spatial correlation of interstitialcies. Our results, which are based on

fewer empirical parameters than that in Ref.¹¹, not only epitomize the origin of instability and atom-scale pathway in the melting process with mathematical rigor but also help to elucidate the origin of "Lindemann particle clusters" and to explain the experimental fact⁷ that ℓ is modulated by both lattice geometry and the profile of interactions.

Paper II is organized as follows: Sect. II is a brief account of the methodology of our interstitialcy model and discuss its symmetry and relations to the 1D model in Paper I; Sect. III uses variational method to work out an approximated solution to the 3D model, where the evolution and correlation of interstitial defects with respect to temperature are investigated; Sect. IV discusses the physical implications of the model solutions where analytical results are compared to data from experiments and simulation; Sect. V summarizes the results in Paper I and Paper II. Appendix A provides an alternative derivation of the defect evolution equation in our argument; Appendix B gives the mathematical details involved in the evaluation of the correlation of defects.

II. MODEL HAMILTONIAN AND ITS QUALITATIVE PROPERTIES

A. Total Hamiltonian

We begin our argument with the Hamiltonian:

$$H = T_A + V_{AA} = H_{\text{vib}} + H_{\text{conf}}; \quad (1)$$

incorporating the kinetic (T_A) and potential (V_{AA}) energies of atoms, treated as the sum of the vibrational Hamiltonian (H_{vib} , the kinetic and elastic potential energies of vibrating atoms²⁰) and the configurational Hamiltonian (H_{conf} , the potential energy of the system when all the atoms are at mechanical equilibrium^{21,22}).

In the three-dimensional (3D) face-centered-cubic (fcc) crystal composed of $2N = 8^{1/3}$ sites and $N = 4^{1/3}$ atoms

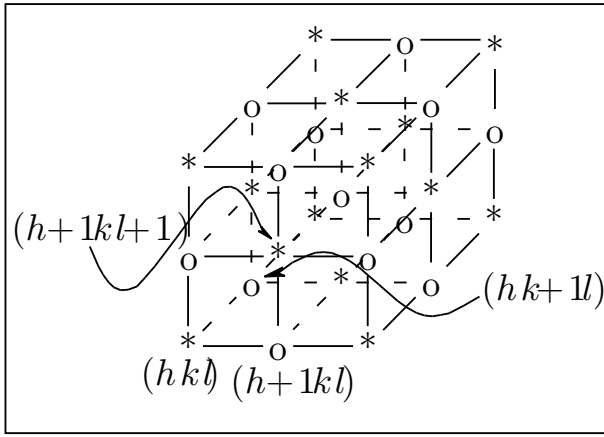


FIG. 1: The way we label the lattice sites ("o") and interstitial sites ("*").

(See FIG. 1), the configurational Hamiltonian reads

$$H_{\text{conf}} = \frac{1}{2} \sum_{h,k,l=1}^N n_{hkl} (J_1 \sum_{j_1, h^0 j_1, j_2, k^0 j_2, j_3, l^0 j_3=1}^N n_{h^0 k^0 l^0} + J_2 \sum_{j_1, h^0 j_1, j_2, k^0 j_2, j_3, l^0 j_3=2}^N n_{h^0 k^0 l^0}) \quad (2)$$

and restrictions

$$n_{h+2, k, l} = n_{h, k+2, l} = n_{h, k, l+2} = n_{h, k, l}; \quad n_{hkl} = N; \quad h, k, l = 1 \quad (3)$$

By writing this Hamiltonian, we set the potential energy of static atom pairs as follows: antibonding energy J_1 for two nearest-neighbor (NN) atoms, bonding energy $J_2 < 0$ for two next-nearest-neighbor (NNN) atoms, and zero otherwise (a generalization of the assumptions in Ref.²³). In order that the NNN distance becomes the bond length, we require that $J_1 > J_2$. Similar to the nomenclature in Paper I, one may call the sites labelled (hkl) where $h+k+l$ is odd (even) as lattice (interstitial) sites, or vice versa. The lattice sites and interstitial sites interpenetrate, as they did in the 1D model in Paper I.

In the 3D fcc case, H_{vib} is taken into consideration in the form of vibrational free energy

$$F_{\text{vib}} = 3N k_B T \log \frac{h h_i}{k_B T}; \quad (4)$$

where k_B is Boltzmann constant, T is absolute temperature, h is Planck constant, h_i is the geometrical mean frequency of the crystal^{20,24}. Note that the formula above is valid in the Debye-Petit limit, the temperature region at which most melting processes take place.

B. Symmetry of the Configurational Hamiltonian

Unlike the 1D exact solution (See Endnote³⁰ in Paper I), we have to treat cases where $J_1 = J_2$ in

the 3D problem in order to model the realistic excitation energy of interstitials in 3D crystals. So it is useful to study the symmetry properties of the configurational Hamiltonian under the transformation: $J_1 \leftrightarrow J_2$. This will shed light on the properties of the "liquid phase" derived from our model Hamiltonian as well as the correlation related to the bonding energy J_2 .

First, by using the transformation $n_{hkl} = 2n_{hkl} - 1$, one could map the model Hamiltonian in Eqn. (2) to the J_1 - J_2 model discussed in magnetism²⁵, where $n_{hkl} = 1$:

$$H_{\text{conf}}(J_1; J_2; f, g) = \frac{1}{8} \sum_{h,k,l=1}^N n_{hkl} (J_1 \sum_{j_1, h^0 j_1, j_2, k^0 j_2, j_3, l^0 j_3=1}^N n_{h^0 k^0 l^0} + J_2 \sum_{j_1, h^0 j_1, j_2, k^0 j_2, j_3, l^0 j_3=2}^N n_{h^0 k^0 l^0}) + \frac{3N}{2} (J_1 + 2J_2); \quad (5)$$

$$n_{h+2, k, l} = n_{h, k+2, l} = n_{h, k, l+2} = n_{h, k, l}; \quad n_{h, k, l} = 0; \quad h, k, l = 1 \quad (6)$$

The partition function corresponding to this configurational Hamiltonian reads: $Q_{\text{conf}}(J_1; J_2; T) = \sum_{f, g} \exp(-H_{\text{conf}}(J_1; J_2; f, g)/k_B T)$.

Second, we notice that the Hamiltonian is invariant under any transformations that swap interstitial sites and lattice sites, i.e. mappings such as $(hkl) \leftrightarrow (h+1kl)$, $(hkl) \leftrightarrow (hk+1l)$, $(hkl) \leftrightarrow (hkl+1)$. (This is called "sublattice symmetry"²⁶.) We make the conventional ansatz²⁶ that there exists a temperature $T^0 > 0K$, above which the partition functions $Q_{\text{conf}}(J_1; J_2; T)$ and $Q_{\text{conf}}(-J_1; J_2; T)$ both preserve the "sublattice symmetry" of the Hamiltonian. In other words, when $T > T^0$, both the $(J_1; J_2)$ and $(-J_1; J_2)$ systems are characterized by equal amount of atoms occupying the lattice sites and interstitials. (It will be shown later in Sect. VI that such a temperature T^0 should be higher than both the melting points of the $(J_1; J_2)$ and $(-J_1; J_2)$ system.) Since the number of atoms occupying either type of sites is $N/2$, we may draw the inference that both partition functions (i.e. $Q_{\text{conf}}(J_1; J_2; T)$ and $Q_{\text{conf}}(-J_1; J_2; T)$) are dominated by terms with configuration f, g satisfying:

$$\sum_{h,k,l=1}^N n_{hkl} = \sum_{h^0, k^0, l^0=1}^N n_{h^0 k^0 l^0} = 0; \quad (7)$$

So the transformation

$$n_{hkl} \leftrightarrow e_{hkl} = (-1)^{h+k+l} n_{hkl} \quad (8)$$

sends one dominant configuration

$$f_{fg} = \sum_{h; k; l=1}^8 X_{hkl}^{fg} = 0; \quad (9)$$

to another dominant configuration

$$f_{eg} = \sum_{h; k; l=1}^8 X_{hkl}^{eg} = 0; \quad (10)$$

in the partition function, and transforms the configurational Hamiltonian in the following way:

$$\begin{aligned} H_{\text{conf}}(J_1; J_2;) \\ \rightarrow H_{\text{conf}}(J_1; J_2; e) \\ = H_{\text{conf}}(J_1; J_2;) + 3N J_1; \end{aligned} \quad (11)$$

where

$$\begin{aligned} H_{\text{conf}}(J_1; J_2; f_{eg}) \\ = \frac{1}{8} \sum_{h; k; l=1}^8 X_{hkl}^{fg} X_{hkl}^{eg} e_{h^0 k^0 l^0} \\ + J_2 \sum_{h^0 k^0 l^0} X_{h^0 k^0 l^0} e_{h^0 k^0 l^0} + \frac{3N}{2} (J_1 + 2J_2); \end{aligned} \quad (12)$$

From the obvious identity:

$$\begin{aligned} \sum_{fg} \exp \left(\frac{H_{\text{conf}}(J_1; J_2; f_{fg})}{k_B T} \right) \\ = \sum_{feg} \exp \left(\frac{H_{\text{conf}}(J_1; J_2; f_{eg})}{k_B T} \right); \end{aligned} \quad (13)$$

we arrive at the result that when $T > T^0$, the configurational free energy ($F_{\text{conf}} = k_B T \log Q_{\text{conf}}$) has the following correspondence due to "sublattice symmetry":

$$\begin{aligned} F_{\text{conf}}(J_1; J_2; T) &= \frac{3N}{2} (J_1 + 2J_2) \\ &= F_{\text{conf}}(J_1; J_2; T) - \frac{3N}{2} (J_1 + 2J_2); \end{aligned} \quad (14)$$

This equation is parallel to Eqn. (12) in Paper I, a formula invariant under the transformation $J_1 \rightarrow -J_1$.

The analysis above reveals that when $T > T^0$, the free energy of the system, up to a trivial ground energy, seems to be only sensitive to J_2 while insensitive to J_1 , because $F_{\text{conf}}(J_1; J_2; T) - 3N J_1 = 2$ even remains unchanged when J_1 changes its sign! This scenario is consistent with the previous description of the liquid phase in the "lattice gas model"²³, that is, the properties of the system is predominantly defined by the NNN attractive bonding energy, and it is unnecessary to take the repulsion at NN distance into account.

Therefore, we have obtained the "liquid phase" solution to our model, which highlights the importance of J_2 at high temperature. In the following section, we will show that for low temperatures $T < T^0$, our model behaves differently as compared to the conclusions above, where different J_1 parameter could change the properties of $F_{\text{conf}}(J_1; J_2; T) - 3N J_1 = 2$ drastically, indicating the loss of sublattice symmetry of the free energy. The interplay of the two energy parameters J_1 and J_2 in low temperatures will prove to be the mechanism that both crystallizes the solid by breaking the "sublattice symmetry" and melts the solid by removing it of this symmetry.

III. THE VARIATIONAL METHOD APPROACH TO THE 3D FCC CRYSTAL

A. Phenomenological Parameter Expansion of the Free Energy Functional and Melting Implications

In our discussion on the 3D fcc crystal, we aim to obtain a solution based on modified mean field approximation (MFA). We first define a random variable called local order parameter

$$L(r) = (-1)^{h+k+l} n_{hkl} = (-1)^{h+k+l} (2n_{hkl} - 1) \quad (15)$$

where site r bears the integer label (hkl) . According to the Landau-Ginzburg theory of MFA²⁷, the free energy functional contributed by configurational Hamiltonian of the 3D fcc model H_{conf} could be expanded phenomenologically as

$$\begin{aligned} F_{\text{conf}}[L(r)] \\ = T S_{\text{conf}}[L(r)] + \frac{1}{2} \sum_{\mathbf{r}} \sum_{\mathbf{h}} L^2(\mathbf{r}) H_1 + \frac{1}{2} \sum_{\mathbf{r}} L^2(\mathbf{r})^2 H_2 + \dots \end{aligned} \quad (16)$$

where $\sum_{\mathbf{r}}$ denotes summation over all the $2N$ sites. $H_1 > 0$ and $H_2 < 0$ are two energy parameters to be

elaborated later. $\beta > 0$ is the phenomenological "do-

main wall energy" coefficient. The configurational entropy $S_{\text{conf}}[L(r)]$, which appears in the equation above, reads as the mixture entropy^{22,24}:

$$S_{\text{conf}}[L(r)] = \int d^3r \left[-\frac{1}{2} \frac{L(r)}{1+L(r)} \log \frac{1}{2} \frac{L(r)}{1+L(r)} - \frac{1}{2} \log \frac{1+L(r)}{2} \right]. \quad (17)$$

$F_{\text{vib}}[L(r)]$ is contributed by vibrations with geometric mean frequencies $\langle h_{\text{li}} \rangle$ (lattice mode) and $\langle h_{\text{ii}} \rangle$ (interstitialcy mode)²⁰, which reads

$$F_{\text{vib}}[L(r)] = \frac{1}{2} \int d^3r \left[\frac{3k_B T}{4} (1 - L^2(r)) \log \frac{\langle h_{\text{li}} \rangle}{\langle h_{\text{ii}} \rangle} + \text{const} \right] \quad (18)$$

when expanded in power series of $1 - L^2(r)$.

Now the total phenomenological free energy functional $F[L(r)]$ reads:

$$F[L(r)] = F_{\text{conf}}[L(r)] + F_{\text{vib}}[L(r)] = \int d^3r f(L(r); r, L(r)) \quad (19)$$

where

$$f(L(r); r, L(r)) = \frac{1}{2} (1 - L^2(r)) H_1 + \frac{1}{2} (1 - L^2(r))^2 H_2 - \frac{3}{2} k_B T (1 - L^2(r)) + k_B T \left[\frac{1}{2} \frac{L(r)}{1+L(r)} \log \frac{1}{2} \frac{L(r)}{1+L(r)} + \frac{1}{2} \log \frac{1+L(r)}{2} \right] + \frac{1}{2} [r L(r)]^2 : \quad (20)$$

and $\frac{1}{4} \log(\langle h_{\text{li}} \rangle / \langle h_{\text{ii}} \rangle) > 0$ is a factor modelling the "lattice softening" effect. By variational methods, we may apply the Euler-Lagrange equation

$$\frac{\partial f(L(r); r, L(r))}{\partial L(r)} = r \frac{\partial f(L(r); r, L(r))}{\partial r L(r)}; \quad (21)$$

to optimize the free energy functional and obtain the equation of motion for $L(r)$ in the following form:

$$(L(r)) = -r^2 L(r); \quad (22)$$

where

$$(L(r)) = H_1 L(r) - 2H_2 L(r) L^2(r) - \frac{1}{2} \frac{3k_B T L(r)}{1+L(r)} - \frac{1}{2} k_B T \tanh^{-1} L(r); \quad (23)$$

For sufficiently low temperature T , the curve $(L(r))$ intersects the positive $L(r)$ -axis at least once (See

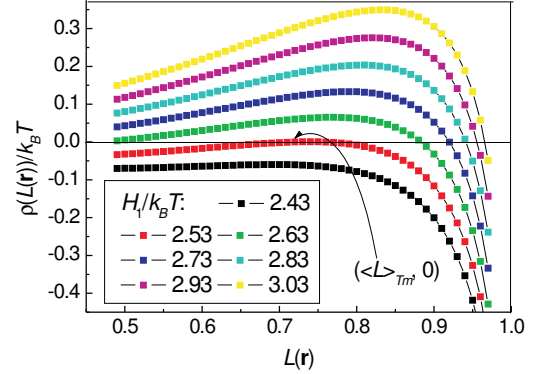


FIG. 2: (color) Local properties of $(L(r)) = k_B T$ near its node: $\langle h_{\text{li}} \rangle$. In this specific case, $H_1 = 6 \langle h_{\text{li}} \rangle / \langle h_{\text{ii}} \rangle = \log(4/3)$. The tangent node $(\langle h_{\text{li}} \rangle_{T_m}; 0)$ is related to the melting point.

FIG. 2), so there is a homogeneous solution $L(r) = \langle h_{\text{li}} \rangle_{T_m} \neq 0$ that makes $(L(r))$ vanish. When $T = T_m$, where T_m satisfies

$$\langle h_{\text{li}} \rangle_{T_m} = 0 \text{ and } \frac{\partial (L(r))}{\partial L(r)} \bigg|_{L(r) = \langle h_{\text{li}} \rangle_{T_m}} = 0$$

simultaneously, the intersection becomes a tangent point and we have the following equations:

$$\begin{aligned} & \frac{1}{2} k_B T_m \left[3 + \frac{1}{1 - \langle h_{\text{li}} \rangle_{T_m}^2} \right] = H_1 - 2H_2 - 3 \langle h_{\text{li}} \rangle_{T_m}^{-1}; \\ & \frac{\frac{1}{2} \langle h_{\text{li}} \rangle_{T_m}^{-1} \tanh^{-1} \langle h_{\text{li}} \rangle_{T_m}}{1 - \langle h_{\text{li}} \rangle_{T_m}^2} = \frac{4}{k_B T_m} H_2 \end{aligned} \quad (24)$$

In FIG. 2, $k_B T_m = H_1 = 2.53$. For temperatures higher than T_m , $(L(r))$ no longer forms an intersection with the positive $L(r)$ -axis, suggesting loss of long-range order. (Note that this instability mechanism is not possible when $H_2 = 0$.) This presents a simple mathematical model of the catastrophe of long-range order.

B. The Cooperation Effect and the H_2 Term

In the MFA scenario,

$$F[\mathbf{L}(r)] = F_{\text{vib}} - TS_{\text{conf}} + \frac{1}{2} \sum_{\mathbf{r}} d^3 \mathbf{r}^n (6J_1 h_{\mathbf{r}} n_{\mathbf{r}^0} i + 12J_2 h_{\mathbf{r}} n_{\mathbf{r}^0} i) + [\mathbf{L}(r)]^2; \quad (25)$$

where $n_{\mathbf{r}} = (\mathbf{r} + 1)/2$, \mathbf{r} and \mathbf{r}^0 are NN sites, \mathbf{r} and \mathbf{r}^0 are NNN sites. One simple-minded approximation yields the result: $h_{\mathbf{r}} n_{\mathbf{r}^0} i = h_{\mathbf{r}} n_{\mathbf{r}^0} i = L^2(\mathbf{r})$. This approximation is equivalent to the ansatz that when the correlation between sites is negligible and $\mathbf{L}(\mathbf{r})$ distribution is uniform, the lattice (interstitialcy) site occupancy is $(1 + \mathbf{j}(\mathbf{r}))/2$ ($(1 - \mathbf{j}(\mathbf{r}))/2$), so that based on the multiplication rule in probability theory²²,

$$\begin{aligned} & h_{\mathbf{r}} n_{\mathbf{r}^0} i \\ &= \frac{1 + \mathbf{j}(\mathbf{r})}{2} \frac{1 - \mathbf{j}(\mathbf{r})}{2} = \frac{1 - L^2(\mathbf{r})}{4} \end{aligned} \quad (26)$$

$$\begin{aligned} & h_{\mathbf{r}} n_{\mathbf{r}^0} i \\ &= \frac{1}{2} \left(h_{\mathbf{r}} n_{\mathbf{r}^0} i_{\text{lattice sites}} + h_{\mathbf{r}} n_{\mathbf{r}^0} i_{\text{interstitialcy sites}} \right) \\ &= \frac{1}{2} \left(\frac{1 + \mathbf{j}(\mathbf{r})}{2} \right)^2 + \frac{1}{2} \left(\frac{1 - \mathbf{j}(\mathbf{r})}{2} \right)^2 \\ &= \frac{1}{2} \frac{1 - L^2(\mathbf{r})}{4} \end{aligned} \quad (27)$$

Such an argument is reasonable when $\mathbf{j}(\mathbf{r})$ is sufficiently close to 1 and the interstitialcy concentration is low enough to obscure the cooperation between defects. When $\mathbf{j} = 0$, the approximation above gives the defect concentration in the form of $(1 - \mathbf{j}(\mathbf{r}))/2 = \exp(-u/2k_B T)$ where $u = 6J_1 - 12J_2$ is the excitation energy of one interstitial defect. This asymptotic behavior of the partition function agrees with the conventional theory of Frenkel defects where excitations of defects are assumed to be spatially independent.

However, the approximation $h_{\mathbf{r}} n_{\mathbf{r}^0} i = h_{\mathbf{r}} n_{\mathbf{r}^0} i$ is far from accurate when the interstitialcy concentration is high and correlation between atoms should be taken with care. By the qualitative analysis of the exact partition function, we see from Eqn. (7) that $h_{\mathbf{r}} n_{\mathbf{r}^0} i$ vanishes in MFA scenario when $T > T^0$, so that $F_{\text{conf}}(J_1; J_2; T) - 3N J_1/2$ is independent of J_1 when $T > T^0$ while employing MFA. However, it does not follow that $h_{\mathbf{r}} n_{\mathbf{r}^0} i = h_{\mathbf{r}} n_{\mathbf{r}^0} i = 0$. In the thermodynamic limit, when $T > T^0$, following the criterion similar to Eqn. (6) in

Paper I, we may write the exact partition function as:

$$\begin{aligned} Q_{\text{conf}}(J_1; J_2; T) &= \sum_{\mathbf{f}, \mathbf{g}} \exp \left(\frac{H_{\text{conf}}(J_1; J_2; \mathbf{f}, \mathbf{g})}{k_B T} \right) \\ &= \sum_{\mathbf{f}, \mathbf{g}} \exp \left(\frac{H_{\text{conf}}(J_1; J_2; \mathbf{f}, \mathbf{g})}{k_B T} \right) \\ &= \frac{2^{2N} \exp \left(\frac{3N}{2k_B T} (J_1 + 2J_2) \right)}{\cosh^{2N} \left(\frac{J_1}{4k_B T} \right) \cosh^{2N} \left(\frac{J_2}{4k_B T} \right)} \\ &= \sum_{\mathbf{r}; \mathbf{s}} g_{\mathbf{r}; \mathbf{s}} \tanh^{\mathbf{r}} \left(\frac{J_1}{4k_B T} \right) \tanh^{\mathbf{s}} \left(\frac{J_2}{4k_B T} \right) \\ &= \frac{2^{2N} \exp \left(\frac{3N}{2k_B T} (J_1 + 2J_2) \right)}{\cosh^{2N} \left(\frac{J_1}{4k_B T} \right)} \sum_{\mathbf{s}} g_{0; \mathbf{s}} \tanh^{\mathbf{s}} \left(\frac{J_2}{4k_B T} \right) \end{aligned} \quad (28)$$

where $g_{\mathbf{r}; \mathbf{s}}$ is the number of loops that contain \mathbf{r} antibonds and \mathbf{s} bonds and \mathbf{r} is an even number. (cf. Appendix A in Paper I) This means $Q_{\text{conf}}(J_1; J_2; T)$ still varies with respect to T when $T > T^0$, and this variation is dependent on the NNN attractive interaction J_2 , indicating that $h_{\mathbf{r}} n_{\mathbf{r}^0} i$ is still non-zero when $T > T^0$.

From the behavior of the exact partition function, we see that the mean NNN correlation is more persistent than its NN counterpart. In other words, the system tends to "preserve" more bonds than assumed in the approximation $h_{\mathbf{r}} n_{\mathbf{r}^0} i = h_{\mathbf{r}} n_{\mathbf{r}^0} i$, which inaccurately states that when interstitialcies are excited, the creation of 6 antibonds is accompanied by annihilation of exactly 12 bonds.

In order to offset the overestimation in the annihilation of bonds, we have to write down

$$\begin{aligned} & 6J_1 h_{\mathbf{r}} n_{\mathbf{r}^0} i + 12J_2 h_{\mathbf{r}} n_{\mathbf{r}^0} i \\ &= 6J_2 + \frac{1}{2} L^2(\mathbf{r}) H_1 + \frac{1}{2} L^2(\mathbf{r})^2 H_2 \end{aligned} \quad (29)$$

where $H_1 = (3/2)(-2J_2 + J_1)$, and the negative coefficient H_2 , which is proportional to J_2 , is to be determined in the next subsection.

C. The Phenomenological Parameters H_2 and Terms of J_1 and J_2

When the concentration of interstitialcies is considerable (about 3%–5%) and the creation of di-interstitialcies (excitation of two interstitial atoms at NNN distance) helps to preserve more NNN atom pairs

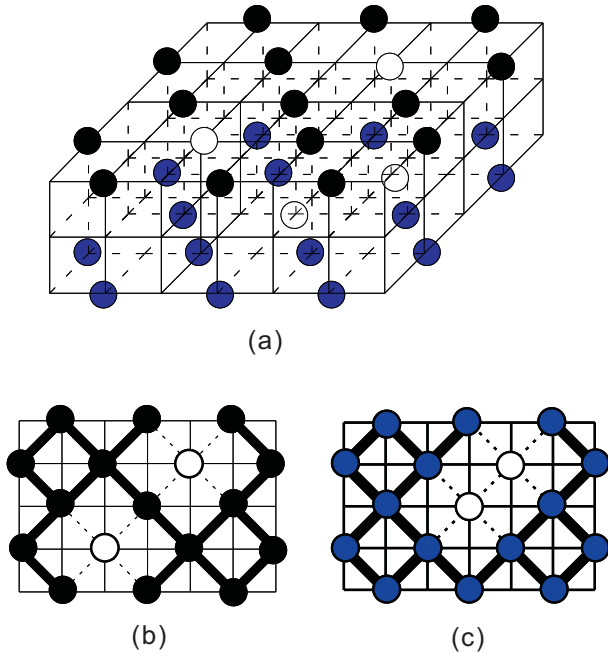


FIG. 3: (a) Two layers in a crystal. In the "upper layer", two holes are separate whereas in the "lower layer", two holes are close. (b) Cross-section view of the "upper layer", with loss of eight bonds (in dashed lines) as compared to a perfect layer. (c) Cross-section view of the "lower layer", with loss of seven bonds (in dashed lines) as compared to a perfect layer. We could see that two close holes save a bonding energy of J_2 (bonds are denoted by thick black lines in (b) and (c)).

than predicted in Eqn. (27). This cooperation effect inherent in the Hamiltonian lowers the energy cost in exciting interstitialcies because di-interstitialcies has less formation energy than that of two interstitialcies at separate distance. Accordingly, we have to correct Eqn. (27) by adding a positive term in order of $O(1 - L^2(r)^2)$ (symmetry and analyticity of the free energy preclude terms including $L(r)$ or $\bar{L}(r)$). One scheme to outline this correction is by estimating the percentage number of occurrence of NNN-contact holes in the lattice sites as

$$\frac{12}{2} \frac{1 - \bar{L}(r)^2}{2} = \frac{3}{8} (1 - L^2(r)^2) \quad (30)$$

where 12 is the coordination number of NNN pairs. (See FIG. 3) This picture shows how "virtual attraction"⁹ between defects is taken into consideration based on probabilistic arguments. The system preserves more bonds than in the simple-minded approximation: when two holes on the lattice sites are close (in NNN contact) instead of being separate, they save the bond energy in amount of J_2 . In total, the saved bonds by stochastic contact of holes lower the system energy in magnitude of $(3=8) \bar{L}(r)^2 (1 - L^2(r)^2)$.

Dynamically speaking, this correction could be also understood by the NNN correlation on the lattice sites. Since the occupancy of lattice sites is approximately

1, the relaxation time of bonds on lattice sites are much longer than that of the bonds on the interstitial sites and the antibonds. So the dissociation of bonds is a "slower reaction" than the creation of antibonds. That is why $\langle n_r n_{r^0} \rangle_{\text{lattice sites}}$ should be greater than $[(1 + \bar{L}(r))^2 = 2]^2$.

Therefore, after considering defect attraction or NNN correlation on the lattice sites, the ensemble average $\langle n_r n_{r^0} \rangle$ should be modified into

$$\langle n_r n_{r^0} \rangle = \frac{1}{2} \left(\frac{1 - L^2(r)}{4} + \frac{3}{8} (1 - L^2(r)^2) \right), \quad (31)$$

so as to account for the crystal's tendency to retain as many NNN atom pairs (bonds) as possible. Since NN sites are scarcely occupied by two atoms simultaneously, NN correlations are immaterial as compared to NNN correlations. In the light of this, we may retain Eqn. (26) in the final expression of free energy functional. Comparing this with Eqn. (29), we have

$$H_2 = \frac{3}{8} J_2 < 0; \quad (32)$$

When spatial inhomogeneity is significant, a domain-wall energy proportional to $[\bar{r} L(r)]^2$ should be taken into account in order to offset the miscalculation () based on the assumption $L(r) = L(r^0) = L(r^{\infty})$. In Eqn. (25), a good estimation of \bar{r} is $a^2 H_1 = 2$ because

$$\begin{aligned} & (2J_1 \langle n_r n_{r^0} \rangle) \\ &= 2 \frac{J_1}{L(r)} \frac{r}{L(r')} \frac{J_1}{L(r)} \frac{r}{L(r')} \frac{J_1}{L(r)} \frac{r}{L(r')} \\ &= J_1 \frac{2pr}{p^2} \frac{r^2}{r^2} \\ &= J_1 (p - r)^2 = J_1 \frac{a^2}{2} [\bar{r} L(r)]^2 \end{aligned} \quad (33)$$

$$\begin{aligned} & (2J_2 \langle n_r n_{r^{\infty}} \rangle) \\ &= 2 \frac{J_2}{p} \frac{L(r'')}{L(r)} \frac{J_2}{p} \frac{L(r'')}{L(r)} \frac{J_2}{p} \frac{L(r'')}{L(r)} \\ &= J_2 a^2 [\bar{r} L(r)]^2; \end{aligned} \quad (34)$$

The total domain-wall energy contributed by the non-vanishing $\bar{r} L(r)$ at site r is thus

$$\begin{aligned} & \frac{1}{4} \left(6 - \frac{1}{2} J_1 \frac{a^2}{2} - J_2 a^2 \right) [\bar{r} L(r)]^2 \\ &= \frac{a^2}{2} H_1 [\bar{r} L(r)]^2; \end{aligned} \quad (35)$$

Here, the factor 1=4 results from the transformation $\bar{r} = 2n_r - 1$, 1=2 is applied to offset the effect of counting one bond twice, 6 is a consequence of coordination number and Pythagoras theorem of the $\bar{r} L(r)$ vector decomposition.

Physically speaking, at low temperatures, the domain wall energy could be interpreted as the energy of dislocations that destroy the continuity of $L(r)$ on the interface.

The $(=2) [r L(r)]^2$ term associated with such rare dislocations contribute little to the total free energy. When temperature is sufficiently high, large fluctuations of $L(r)$ will be commonplace and the gradient term will become indispensable if we want to evaluate the total free energy correctly. (It should be emphasized that the vibration term containing $\nabla^2 L(r)$ arises from entropy effect and does not contribute to domain wall energy. Even when the distribution of $L(r)$ is inhomogeneous, the average vibrational energy for every degree of freedom is the same, regardless of vibrational frequency.)

D. "Chemical Equilibrium" and its Demise to Locally Isotropic Instability

The physical implications behind the mathematical model outlined in Sect. III. A provide much more information about the melting pathway.

First, for $T < T_m$, we find that $[hLi_T] = 0$ is equivalent to the "chemical equilibrium" condition:

$$\frac{1}{1 + [hLi_T]} = \frac{[\text{defective cell}]}{[\text{non-defective cell}]} = e^{-\frac{\tau}{k_B T}}; \quad (36)$$

Here, $[]$ denotes equilibrium concentration, and

$$\tau = 2(H_1 - 3k_B T) [hLi_T] - 4H_2 [hLi_T]^2 [hLi_T]^2 - 1 \quad (37)$$

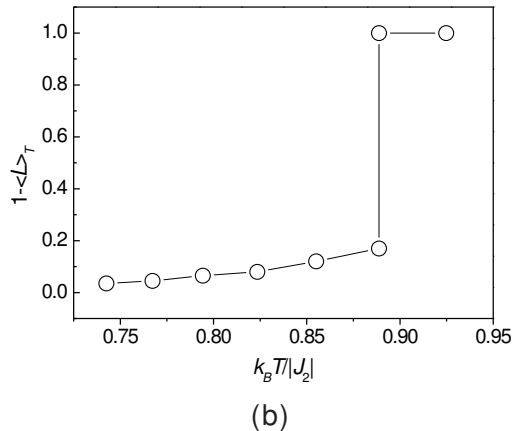
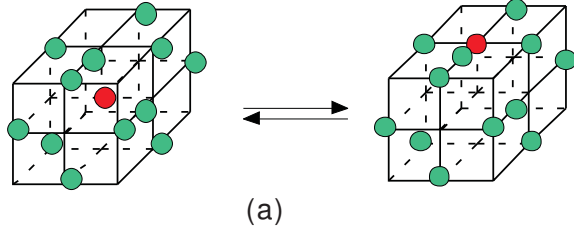


FIG. 4: (a) "Chemical equilibrium" between non-defective (left) and defective (right) cells at $T < T_m$. (b) $1/(1 + [hLi_T])$ versus $k_B T = J_2 J$ when $H_1 = 6 J_2 J$, $\log(4=3)$. There is a catastrophe when $k_B T = J_2 J = 0.89$, corresponding to the melting point.

denotes the energy difference between two types of crystal cells: the defective cell incorporating (in the statistical parlance) more than one (inclusive) interstitialcy and the non-defective cell including less than one interstitialcy (FIG. 4 (a)). (In Appendix A, we will derive the form of τ from a perspective independent from the arguments in previous subsections.) This dynamical equilibrium is achieved by stochastic creation and annihilation of interstitialcies, or vividly speaking, the collisions in a dilute "gas" of interstitial monomers and interstitial oligomers, in search of a minimal free energy corresponding to an optimized long-range order parameter hLi_T (FIG. 4 (b)).

Second, we notice that the "collision process" above causes a fluctuation of $L(r)$, governed by Eqn. 22 that resembles the equation for a globally neutral plasma when $T = T_m$. ($L(r)$) changes sign as $L(r)$ varies in the vicinity of hLi_T , which is analogous to the coexistence of positive and negative charges in a plasma.) The Green function of fluctuation response $G(r; r')$ satisfy

$$\frac{\nabla^2}{a^3} r^2 + \frac{\partial (L(r))}{\partial L(r)} G(r; r') = -k_B T \delta(r - r'); \quad (38)$$

where $\delta(r - r')$ is the Dirac delta function (See Appendix B for the derivation of the Green function). For sufficiently low temperature $T < T_m$, the partial derivative in the equation above is always negative, so $G(r; r')$ is a propagator that decays exponentially and guarantees the stability of the homogeneous distribution $L(r) = hLi_T$. However, as T approaches T_m from below, it is possible that $\partial (L(r)) / \partial L(r) > 0$ for certain values of $L(r)$ not far from hLi_T , which results from a non-Gaussian perturbation (Appendix B) to the homogeneous distribution. Upon $T = T_m$, which is defined in Eqn. 24, $(L(r))$ no longer changes sign in the vicinity of hLi_T , and could be expanded as $(L(r)) = \frac{1}{2} (r - hLi_T)^2 + \frac{1}{3} (r - hLi_T)^3 + \dots$ in the vicinity of hLi_T , where $(r) = L(r) - hLi_T$.

Physically speaking, this expansion of $(L(r))$ infers that the uniform distribution $L(r) = hLi_T$ is unstable when there is a radial symmetric perturbation (Y_{00} wave) of $L(r)$ judging the Gaussian theorem:

$$\begin{aligned} & \int_V \nabla^2 L(r) dV = \oint_S \nabla L(r) \cdot d\mathbf{S} \\ & = \int_V \frac{\partial (L(r))}{\partial L(r)} dV > 0; \quad L(r) > 0 \\ & < 0; \quad L(r) < 0 : \quad (39) \end{aligned}$$

When a perturbative Y_{00} wave initiates, the surface integral boosts when the spherical volume is increased, and $L(r)$ diverges along the radial direction. Anisotropic Y_{lm} modes do not apparently encounter an $L(r)$ singularities from the equation above because for these modes, there is no such a causal relationship between the surface integral divergence and $L(r)$ divergence in the radial direction.

It can be verified mathematically that anisotropic Y_{lm} modes are quenched in order of r^{-1} in the short range and do not account for the instability. This is because (r)

satisfies:

$$r^2 \omega(r) = \omega^2(r) + \omega^3(r) \quad (40)$$

For anisotropic excitations, where the asymptotic behavior is $\omega(r) \sim Y_{lm}(r)/r^l$, $r = |r| \neq 0$ (the original point of r is placed at the center of excitation), $l > 0$, we find

$$\begin{aligned} \omega(r) = & \frac{l(l+1)}{r^2} \omega(r) + \frac{\omega^2(r) Y_{lm}(r)}{r} \\ & + \frac{\omega^3(r) Y_{lm}^2(r)}{r^2} \\ & \frac{l(l+1)}{r^2} \omega(r); \end{aligned} \quad (41)$$

where $\omega(r) = |r|^{-l} \omega(r)$.

$$\omega(r) \sim r^{-l} \quad l \neq 0; r \neq 0 \quad (42)$$

Meanwhile, Y_{00} wave has the following asymptotic behavior:

$$\omega(r) \sim \frac{2}{3} \quad r \neq 0 \quad (43)$$

Therefore, isotropic excitation dominates the instability mechanism at T_m , because all the Y_{lm} ($l > 0$) modes are quenched by the Y_{00} mode in the short range.

E. Relations with Born and Lindemann Criteria: "Lindemann Particle Clusters" Revisited

In the context of instability induced by locally isotropic excitations, "quasi-neutrality" in the "plasma" is attained by establishing $L(r) > 0$ and $L(r) < 0$ domains, each in diameter of $\sqrt{2} a H_1^{-2/3} (2/3 k_B T_m)^{-1/2}$ (Appendix B elaborates on this estimation), which is the average size of the locally isotropic excitations of atom clusters. These highly cooperative and energetic atom clusters gives rise to a catastrophe of global long-range order at T_m :

$$|L(r)| \neq 0; \quad T \neq T_m \quad 0; \quad (44)$$

The vanishing long-range order $|L(r)|$ at temperatures higher than T_m casts the system to sublattice symmetry.

Such locally isotropic excitations near T_m form one possible interpretation for the origin of Lindemann particles and their aggregation. They also provide convincing evidence that both Lindemann and Born criteria should be satisfied by such atom clusters: (1) The average atom displacement in these clusters exceeds a_L (a_L : the critical Lindemann ratio) which is the average value of energetic and inert atoms combined at T_m ; (2) The excitations of such clusters are isotropic in nature, so for the

Born term of the elastic moduli, the hydrostatic isotropy is guaranteed: $C_{xxxx}^B = C_{xyyy}^B$, which means that there is only normal stress of the same magnitude in all directions in response to strain. In this respect, such atom clusters could be regarded as pre-liquid droplets. Since the correlation of fluctuations always form nearly spherical clusters and spheres cannot fill the space completely, it is evident that the solid shear modulus on the whole does not approach zero as T tends to the superheating limit T_m .

Upon $T = T_m$, there are catastrophes of both shear modulus and atom displacement due to avalanche of the energetic and locally isotropic atom clusters that satisfy Lindemann and Born relations simultaneously.

IV. DISCUSSIONS

From the arguments outlined above, we provided answers to why, how and when a crystal melts.

The crucial instability mechanism (why) of melting is found to be the cooperative creation of interstitialcies that caused the avalanche of displaced atoms. In the melting point formula Eqn. (24), it is clear that the first order transition disappears when H_2 is zero. The cooperation between the interstitialcies proves to lower the energy cost to excite defects thereby paving the way for destructing the long range order in the lattice. For fixed bonding energy J_2 and lattice softening, T_m is lowered when H_2/H_1 ratio is enhanced, which is in accordance with the 1D exact solution which relates high H_2/H_1 ratio to great disorder.

To justify this, we will prove the following

Theorem:

$$\frac{\partial T_m}{\partial H_1} \bigg|_{H_2} > 0 \quad (45)$$

in the 3D fcc case.

Proof: From Eqn. (24), pick $H_1 i_{T_m} > 0$, we may draw the following conclusion:

$$\begin{aligned} & \frac{\partial}{\partial H_1 i_{T_m}} \frac{H_1 - 3k_B T}{H_2} \\ = & \frac{4 H_1 i_{T_m} - 1}{H_1 i_{T_m} - 1} \frac{H_1^2 i_{T_m}^2 \tanh^{-1} H_1 i_{T_m}}{H_1^2 i_{T_m}^2 \tanh^{-1} H_1 i_{T_m}} \frac{1}{i_2} \\ & \int_{H_1 i_{T_m}}^{\infty} \frac{8x^4 dx}{(1-x^2)^3} \\ & < 0: \end{aligned} \quad (46)$$

Therefore, we have the following logic chain:

$$\frac{J_2}{T_m} \text{ is fixed } E_{qn}^{(24)} \propto \frac{1}{hL_{T_m}} \quad \Rightarrow \quad \frac{H_1}{T_m} \propto \frac{3k_B T_m}{J_2} \quad \Rightarrow \quad \frac{H_1}{T_m} \propto \frac{J_2}{T_m} :$$

Thus,

$$\frac{\partial T_m}{\partial H_1} \propto \frac{J_2}{H_1^2} > 0 \quad (47)$$

is evident.

That is to say, T_m is not only determined by the bonding energy related to H_2 , but is also modulated by the difficulty to create interstitialcies, which is signified by H_1 . Unlike the liquid-gas phase transition involving the thorough dissociation of neighboring atom pairs, in which J_2 plays a decisive role in determining the boiling point, the solid-liquid phase transition is possible when destruction of the lattice structure and the excitation of interstitialcies are both highly encouraged. Therefore, some materials could have high boiling points and "disproportionately" low melting points, if they have a large J_2 and a small J_1 . (This may have shed light on the peculiar behavior of Ga and In, two metals that melt near room temperature and boil at thousands of Kelvins, although neither metal falls into the category of 3D fcc crystals.) The lattice softening > 0 is also conducive to melting in that $H_1 \propto \frac{3k_B T_m}{J_2} < H_1$ enhances the apparent J_2/J_1 ratio. From this we know that the atom displacement and lattice softening are mutually complementary and this rule underlies the intrinsic relation between Lindemann and Born criteria.

The atom-scale pathway (how) of melting is spatial correlations of atom occupancy fluctuations. The correlation-response scheme proves to be the effective way to transfer information in both 1D and 3D cases. The anomalous sinusoidal correlation wave results from the non-Gaussian fluctuations of atoms. In Ref.⁵, it was observed that melting is preceded by the non-Gaussian behavior of atom displacement, but the causal relationship between the deviation from normal distribution and melting was not explicitly established. This paper presents a clear demonstration of this causality in Sect. V 4. From the conclusions in that subsection, we may find the critical diameter of energetic atom clusters for the example shown in FIG. 3 (b): $r_{min} = 15.03a$, and the spherical volume $(r_{min})^3/6 = 1780a^3$ which contains 890 atoms in average. This forms a good comparison with the statement in Ref.⁵ that the collaborative and energetic "Lindemann particle" clusters consist of $10^2 \sim 10^3$ atoms.

The melting point (when) is defined in Eqn. 24 and it is shown to be the superheating limit predicted by Born and Lindemann criteria simultaneously. When rewritten,

the melting formula takes the form

$$T_m = \frac{3J_2 J_1 hL_{T_m}^3}{2k_B \frac{hL_{T_m}}{1 - hL_{T_m}^2} \tanh^{-1} hL_{T_m}} < \frac{9J_2 J_1}{4k_B} \quad (48)$$

The inequality results from the following Theorem :

$$\frac{2}{3} < \frac{\frac{hL_{T_m}}{1 - hL_{T_m}^2} \tanh^{-1} hL_{T_m}}{hL_{T_m}^3} \quad (49)$$

Proof: Pick $hL_{T_m} > 0$;

$$\begin{aligned} & \frac{hL_{T_m}}{1 - hL_{T_m}^2} \tanh^{-1} hL_{T_m} - \frac{2}{3} hL_{T_m}^3 \\ &= \int_0^{hL_{T_m}} \frac{2x^4 - 2x^2}{(1 - x^2)^2} dx > 0 \end{aligned} \quad (50)$$

If we use $T_m = 1.2T_E$ as an estimation⁵, where T_E is the equilibrium melting point of crystals with surfaces, we can check the reasonability of the formula above by the following table:

	fcc-Cu	fcc-Ar
$H = H_{gas} - H_{solid} = kJ \cdot mol^{-1}$	338.32	7.74
$J_2/J_1 = \frac{H}{6N_A} = J$	9.37 $\cdot 10^{-20}$	2.14 $\cdot 10^{-21}$
$T_E = K$	1356.6	83.78
$T_m = 1.2T_E = K$	1627.92	100.5
$\frac{9J_2 J_1}{4k_B} = K$	15277	349
hL_{T_m}	0.93	0.81
$\frac{1}{2} \frac{1 - hL_{T_m}^2}{hL_{T_m}}$	0.035	0.095

The data suggest that melting triggered when the concentration of interstitial defects is very low but still high enough to induce correlation and cooperation. For noble gases Ne, Ar, Kr, Xe, Rn, the interaction mode is the well-known van der Waals force and they assume a fcc structure in the solid state, so they share the same dimensionless parameters J_2/J_1 and T_m in our model. Hence they should have, in principle and in practice, the same dimensionless values: hL_{T_m} , $J_2/J_1 = T_m$, and $\frac{1}{2} \frac{1 - hL_{T_m}^2}{hL_{T_m}} = K/a^2$, where K is elastic constant, a is bond length respectively.

In our model, $k_B T_m = J_2/J_1$ is a function of hL_{T_m} that varies slowly with respect to hL_{T_m} . The variation itself

betrays that ϵ_L is not a universal constant independent of interaction force, and the slow variation explains the reason why similar materials have nearly identical ϵ_L 's.

The drawbacks of the current model reside in the approximation. The relations $H_2 = (3/8)J_2$, $\epsilon = a^2 H_1/2$ and the representation of ϵ_{min} are obtained by bold assumptions and simplifications. However, judging the physical origin of the collaborative effect and domain wall energy, it is clear that $H_2 < 0$, $\epsilon > 0$ is not questionable even when they are evaluated exactly. $\epsilon_3 > 0$ is also guaranteed in all cases:

Theorem: $\epsilon_3 > 0$ at $T = T_m$

Proof:

$$\begin{aligned} \epsilon_3 &= \frac{\epsilon^3}{\epsilon^3 L(r)} [2H_2 L^3(r) + k_B T_m \tanh^{-1} L(r)] \\ &= 12H_2 + 2k_B T_m \frac{4L^2(r) [1 - L^2(r)] + 1}{(1 - L^2(r))^3} \\ &= k_B T_m \left(\frac{3}{L^3(r)} \frac{L(r)}{1 - L^2(r)} \tanh^{-1} L(r) \right. \\ &\quad \left. + 2 \frac{4L^2(r) [1 - L^2(r)] + 1}{(1 - L^2(r))^3} \right) \\ &= \frac{48k_B T_m}{L^3(r)} \int_0^{L(r)} \frac{x^4 dx}{(1 - x^2)^4} > 0 \end{aligned} \quad (51)$$

^p This justifies the representation of $\frac{2aH_1^2}{2\epsilon_3 k_B T_m} > 0$.

Fortunately, the effectiveness of most of the inferences in our model depend on the sign of such parameters instead of their exact values, so the related physical picture of melting will not change even if parameter values are modified by better methods.

V. CONCLUSIONS

In Papers I and II, we have provided the detailed arguments involving the solution of the melting process in the 1D atom chain and 3D fcc crystal. In both cases, we have used independent approaches to obtain the same result. The solution of the model shows that the phenomenological concerns in Lindemann and Born criteria: atom displacement and lattice softening alone are

only conducive to, but not decisive in the melting process, and they two serve as a reflection of the underlying short-range cooperative creation of interstitialcies, which is crucial for the feasibility of a first-order phase transition marked by catastrophes of both rigidity and displacement. The medium range correlation between interstitial clusters near the melting point triggers an heterogeneous instability and could be deemed as pre-liquid droplets satisfying Born and Lindemann criteria simultaneously.

Acknowledgments

This work is supported by National Natural Science Foundation of China and 973 project.

APPENDIX A: THE DEFECT CONCENTRATION EQUATION REVISITED

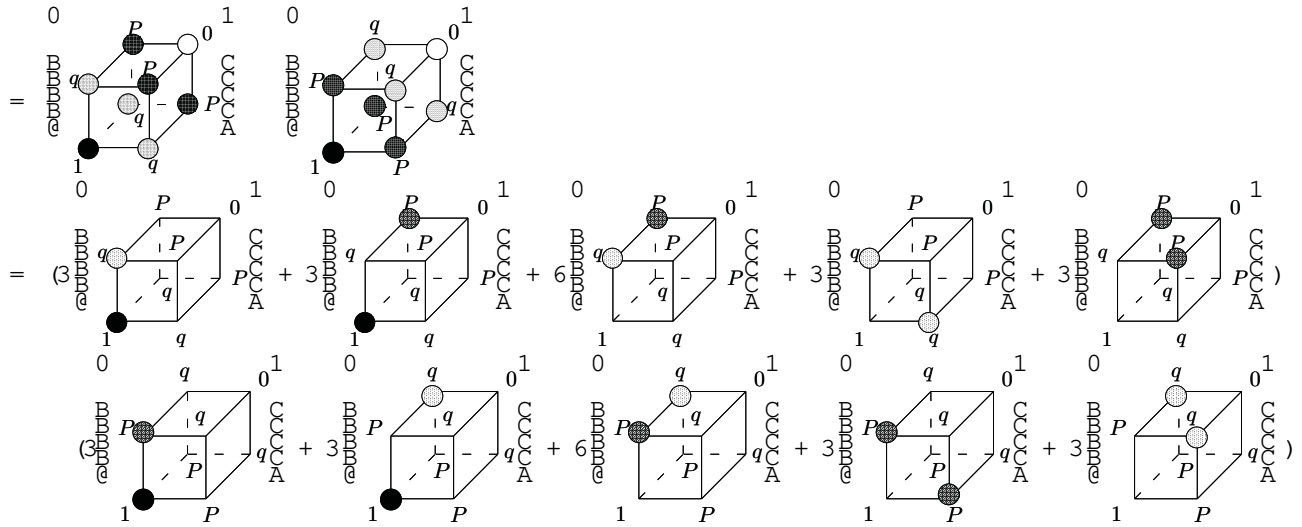
1. \ChemicalEquilibrium" of Cells in the Absence of H_2 and

In this subsection, we will provide an alternative derivation of the \chemical equilibrium" condition Eqn. (36) so as to check Eqn. (22). For simplicity, vibration is provisionally neglected in the following few paragraphs.

We set out to evaluate the configurational energy difference between defective and non-defective cells when $(1 + jL_{ij})/2 = P$ and $(1 - jL_{ij})/2 = q$. Here, P is the probability that a site is occupied \correctly" and $q = 1 - P$. We use the following diagrams to aid calculation, bearing in mind that each edge in the cube below is shared by four cubes and each diagonal line on the surface of the cube is shared by two cubes. Every vertex of the cube (shared by eight cubes) is labelled by the site occupancy { the probability that the corresponding site is occupied by an atom.

If NNN correlation is negligible,

$$\begin{aligned} &\frac{\pi}{4} \\ &= \frac{1}{4} (\pi_{\text{defective cell}} - \pi_{\text{non-defective cell}}) \end{aligned} \quad \begin{aligned} &(A1) \\ &(A2) \end{aligned}$$



$$\begin{aligned}
 &= (3 \frac{J_1}{4} q + 3 \frac{J_2}{2} P + 6 \frac{J_1}{4} qP + 3 \frac{J_2}{2} q^2 + 3 \frac{J_2}{2} P^2) \\
 &\quad (3 \frac{J_1}{4} P + 3 \frac{J_2}{2} q + 6 \frac{J_1}{4} Pq + 3 \frac{J_2}{2} P^2 + 3 \frac{J_2}{2} q^2) \\
 &= \frac{3}{4} (J_1 + 2J_2) (P - q) \\
 &= \frac{3}{4} (J_1 + 2J_2) \ln \frac{P}{q} \quad (A3)
 \end{aligned}$$

This value is equal to $(1=4) \ln$ because for each cube, the state of $2^3 = 8$ atoms are definite, marked by occupancy 1 and 0 respectively. Therefore, the dynamical equilibrium between the two types of cell requires that

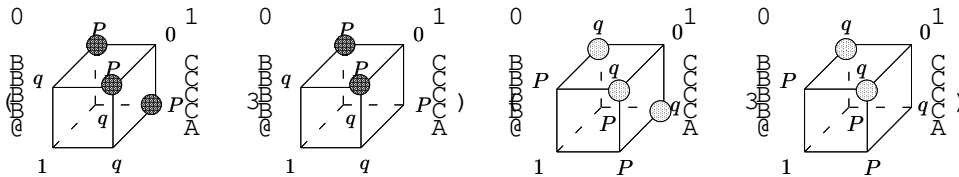
$$\frac{q}{P} = \frac{1}{1 + \ln \frac{P}{q}} = \exp \left(- \frac{2H_1 \ln \frac{P}{q}}{k_B T} \right) \quad (A4)$$

where $H_1 = (3=2) (J_1 - 2J_2)$. This agrees with Eqs. (22)

and (36) when term associated with H_2 , are neglected. As $\ln \frac{P}{q} \neq 1$, Eqn. (A4) implies $q \approx \exp(-u/2k_B T)$, which agrees with the well-established theory of Frenkel defects. Here, $u = 4H_1$ is the excitation energy of an interstitial defect.

2. \ChemicalEquilibrium involving H_2 and

When $\ln \frac{P}{q}$ is sufficiently far from unity, the cooperation and correlation between NNN atoms could not be neglected. We can estimate such NNN correlation by postulating that the three sites that are NNN neighbor to the probability-one-occupied site tend to be occupied or be unoccupied simultaneously. Considering this cooperative effect, we should modify $(1=4) \ln$ by adding the following diagram contributions:



$$\begin{aligned}
 &= \frac{3J_2}{2} P^3 - 3 \frac{J_2}{2} P^2 q - \frac{3J_2}{2} q^3 + 3 \frac{J_2}{2} q^2 P \\
 &= - \frac{3J_2}{2} (P - q) P q \\
 &= - \frac{3J_2}{8} \ln \frac{P}{q} \ln \frac{P}{q} \quad (A5)
 \end{aligned}$$

Accordingly, the chemical equilibrium condition now reads:

$$\begin{aligned}
 &\frac{1}{1 + \ln \frac{P}{q}} \\
 &= \exp \left(- \frac{1}{k_B T} [2H_1 \ln \frac{P}{q} + \frac{3J_2}{8} (\ln \frac{P}{q})^2] \right) \quad (A6)
 \end{aligned}$$

where $H_2 = (3/8)J_2$, in perfect agreement with Eqs. (22) and (36) leaving alone the vibration term.

The contribution from vibrations could be easily considered by the transformation $4H_1 \rightarrow 4H_1 - 3k_B T \log(h_{1i} = h_{1i})$ because averaging speaking, exciting one Frenkel pair changes one eigenfrequency from h_{1i} to h_{1i} .

The chemical equilibrium between defective and non-defective cells is reached by stochastic motion of interstitialcies, which guarantees sufficient chaos of NN pair states (a corollary of short relaxation time of NN atom pairs) thereby supporting the former argument that holds NN correlation to be negligible. In the meantime, NNN atom pairs have considerably long relaxation time and their correlation will lead to spatial inhomogeneity, which is to be elaborated in the Appendix B.

APPENDIX B: THE SPATIAL CORRELATION OF EXCITATIONS IN DETAIL

1. The Green Function

In this subsection, we establish the equation of order correlation functions and obtain expressions for the correlation length at low temperatures. We now start to work with the unit system where $a = 1/2$. In this special system, d^3r could be interpreted as the summation over the $2N$ sites as well as a volume integration.

The equation of $L(r)$ spatial correlation Green function is obtained by the following procedure²⁶:

(1) We introduce a phenomenological external field $H(r)$ and rewrite the free energy functional as

$$F[L(r); H(r)] = F[L(r)] - d^3r H(r) L(r); \quad (B1)$$

(2) We use functional derivative to verify

$$\begin{aligned} & \frac{\delta^2 F[L(r); H(r)]}{\delta H(r) \delta H(r')} \\ &= k_B T \frac{1}{Q} \frac{\delta^2 Q}{\delta H(r) \delta H(r')} = \frac{1}{Q} \frac{\delta Q}{\delta H(r)} \frac{1}{Q} \frac{\delta Q}{\delta H(r')} \\ &= \frac{1}{k_B T} [hL(r) L(r') - hL(r) i hL(r') i] \\ &= \frac{1}{k_B T} G(r; r') \end{aligned} \quad (B2)$$

where $Q = \exp(-F/k_B T)$.

(3) On the other hand, $F[L(r); H(r)] = L(r) = 0$ implies that

$$r^2 L(r) - (L(r)) - H(r) = 0; \quad (B3)$$

Recalling that

$$\frac{hL(r) i}{H(r')} = \frac{\delta^2 F[L(r); H(r)]}{\delta H(r) \delta H(r')} \quad (B4)$$

and

$$\frac{H(r)}{H(r')} = (r - r'); \quad (B5)$$

we apply functional differentiation to obtain:

$$\begin{aligned} 0 &= \frac{r^2 L(r) - (L(r)) - H(r)}{H(r')} \\ &= \frac{1}{k_B T} r^2 \frac{\partial (L(r))}{\partial L(r)} - G(r; r') = (r - r'); \end{aligned} \quad (B6)$$

which is equivalent to Eqn. (38). It is clear that $G(r; r')$ is the propagator of Eqn. (22).

For $T \rightarrow T_m$, where T_m is defined by Eqn. (24), $(L(r))$ is almost linear in the vicinity of hL_{1T} , so $\partial (L(r)) / \partial L(r)$ is almost a constant 1 even when fluctuation is considered. The solution of the propagator is then

$$\begin{aligned} G(r; r') &= \frac{k_B T}{4r} e^{-r/r'}; r = |r - r'|; \\ \epsilon_T &= \frac{1}{1} \end{aligned} \quad (B7)$$

However, for $T \rightarrow T_m$, the linearity of $(L(r))$ in the vicinity of hL_{1T} is lost and the corresponding non-Gaussian fluctuations of $L(r)$ in different magnitudes have different propagation modes and correlation length. A $|L(r)| > hL_{1T}$ fluctuation decays exponentially ($\partial (L(r)) / \partial L(r) < 0$), but $|L(r)| < hL_{1T}$ fluctuations could be propagated in the form of a cosinusoidal wave ($\partial (L(r)) / \partial L(r) > 0$). The mean wavelength will be estimated in the next subsection.

Such fluctuation propagation is a consequence of plasma instability at T_m , and gives rise to collaborative atom clusters, the shape of which is nearly spherical, for the reason outlined in the next subsection.

2. The Correlation Functions Near T_m

The mean wavelength of $L(r)$ fluctuation correlation could be estimated by the following steps:

(1) Define the Fourier expansion of (r) as

$$(r) = \sum_K (K) e^{iK \cdot r} \quad (B8)$$

so that the complex conjugate of (K) is $(-K)$ and that

$$r(r) = \sum_K iK (K) e^{iK \cdot r} \quad (B9)$$

and expand the free energy functional in series of (K) in a volume $V = 2N$ which contains $2N$ sites:

$$\begin{aligned}
F &= F_{\text{hLi}_{T_m}} + \int d^3r \frac{1}{3} \nabla^2 (r^2) \\
&\quad + \frac{1}{4} \nabla^4 (r^2) + \frac{1}{2} [\nabla^2 (r^2)]^2 \\
&= F_{\text{hLi}_{T_m}} + \int d^3r \sum_{\mathbf{K}} \frac{1}{2} (i\mathbf{K}) \cdot (i\mathbf{K}^0) (\mathbf{K}) \cdot (\mathbf{K}^0) e^{i(\mathbf{K} + \mathbf{K}^0) \cdot \mathbf{r}} \\
&\quad + \frac{2}{3} \sum_{\mathbf{K}_1, \mathbf{K}_2, \mathbf{K}_3} (\mathbf{K}_1) \cdot (\mathbf{K}_2) \cdot (\mathbf{K}_3) e^{i(\mathbf{K}_1 + \mathbf{K}_2 + \mathbf{K}_3) \cdot \mathbf{r}} \\
&\quad + \frac{3}{4} \sum_{\mathbf{K}_1, \mathbf{K}_2, \mathbf{K}_3, \mathbf{K}_4} (\mathbf{K}_1) \cdot (\mathbf{K}_2) \cdot (\mathbf{K}_3) \cdot (\mathbf{K}_4) e^{i(\mathbf{K}_1 + \mathbf{K}_2 + \mathbf{K}_3 + \mathbf{K}_4) \cdot \mathbf{r}}; \\
&= F_{\text{hLi}_{T_m}} + V \sum_{\mathbf{K}} \frac{1}{2} K^2 j(\mathbf{K})^2 + \frac{V}{3} \sum_{\mathbf{K}_1 + \mathbf{K}_2 + \mathbf{K}_3 = 0} (\mathbf{K}_1) \cdot (\mathbf{K}_2) \cdot (\mathbf{K}_3) \\
&\quad + \frac{V}{4} \sum_{\mathbf{K}_1 + \mathbf{K}_2 + \mathbf{K}_3 + \mathbf{K}_4 = 0} (\mathbf{K}_1) \cdot (\mathbf{K}_2) \cdot (\mathbf{K}_3) \cdot (\mathbf{K}_4)
\end{aligned} \tag{B10}$$

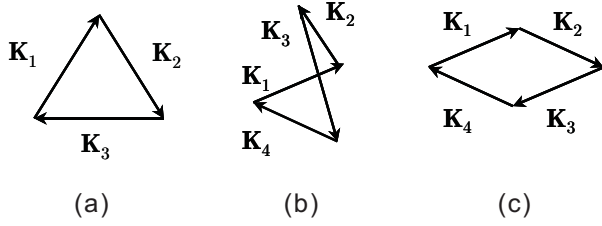


FIG. 5: (a) $\mathbf{K}_1 + \mathbf{K}_2 + \mathbf{K}_3 = 0$ where $j_1 = j_2 = j_3$. (b) $\mathbf{K}_1 + \mathbf{K}_2 + \mathbf{K}_3 + \mathbf{K}_4 = 0$ where $j_1 = j_2 = j_3 = j_4$. In general, such "out-of-plane" term $(\mathbf{K}_1) \cdot (\mathbf{K}_2) \cdot (\mathbf{K}_3) \cdot (\mathbf{K}_4)$ does not contain $j(\mathbf{K}_1)^2$ explicitly. (c) "In-plane" four wave vectors. In such case, $(\mathbf{K}_1) \cdot (\mathbf{K}_2) \cdot (\mathbf{K}_3) \cdot (\mathbf{K}_4) = j(\mathbf{K}_1)^2 j(\mathbf{K}_2)^2$.

where $K = j$.

(2) Evaluate $j(\mathbf{K})^2$ by

$$j(\mathbf{K})^2 = \frac{\int d^3r e^{i\mathbf{K} \cdot \mathbf{r}} e^{-\frac{F}{k_B T_m} Q} Q}{\int d^3r e^{-\frac{F}{k_B T_m} Q} Q} \tag{B11}$$

Based on the assumption that the fluctuation wave has a definite wave length 2π , we can assert that only $j = 1$ terms dominate the sum in Eqn. B10 (See FIG. 5 and Ref.²⁹) and carry out the summation only on equilateral polygons of K . This results in

$$\begin{aligned}
&F_{\text{hLi}_{T_m}} \\
&= V \sum_{\mathbf{K}} \frac{1}{2} K^2 j(\mathbf{K})^2 + O(K^3) \\
&\quad + \frac{V}{4} \sum_{\mathbf{K} = \mathbf{K}^0} j(\mathbf{K})^2 j(\mathbf{K}^0)^2 \tag{B12}
\end{aligned}$$

where "out-of-plane" contributions of $(\mathbf{K}_1) \cdot (\mathbf{K}_2) \cdot (\mathbf{K}_3) \cdot (\mathbf{K}_4)$ (See FIG. 4 (b)) are assumed to be cancelled by phase randomness. By using the density of states in K -space, one finds

$$\begin{aligned}
&\sum_{\mathbf{K}} j(\mathbf{K}^0)^2 \\
&= \frac{V}{(2\pi)^3} \int d^3K j(\mathbf{K}^0)^2 \delta(K - K^0) \\
&= \frac{V}{6\pi^2} j(\mathbf{K}^0)^2 \int_0^{K^0} K^3 dK \\
&= \frac{V c^2 + 3}{3^2} \frac{j(\mathbf{K}^0)^2}{3} \text{ when } K = c^{-1} \tag{B13}
\end{aligned}$$

and

$$\begin{aligned}
&\sum_{\mathbf{K} = \mathbf{K}^0} j(\mathbf{K})^2 j(\mathbf{K}^0)^2 \\
&= \frac{V c^2 + 3}{3^2} \sum_{\mathbf{K} = \mathbf{K}^0} j(\mathbf{K})^4; \tag{B14}
\end{aligned}$$

which leads to the approximation:

$$\begin{aligned}
& \left(\frac{V}{k_B T_m a^3} \frac{1}{2} K^2 j(K)^2 + O \left(\frac{1}{K^3} \right) + \frac{3}{4} \frac{V c c^2 + 3}{3^2 3} j(K)^4 \right) \\
& = \frac{V}{k_B T_m} \frac{1}{2} K^2 j(K)^2 + O \left(\frac{1}{K^3} \right) + \frac{3}{4} \frac{V c c^2 + 3}{3^2 3} j(K)^4 + O \left(\frac{1}{K^6} \right) \\
& = \frac{2k_B T_m}{V K^2} \frac{1}{4k_B T_m} \frac{V c c^2 + 3}{3^2 3} \frac{3}{4} \frac{2k_B T_m a^3}{V K^2} \frac{1}{K^2} + O \left(\frac{1}{K^7} \right) \quad (B15)
\end{aligned}$$

$$\begin{aligned}
& \left(\frac{V}{k_B T_m} \frac{1}{2} K^2 j(K)^2 + O \left(\frac{1}{K^3} \right) + \frac{3}{4} \frac{V c c^2 + 3}{3^2 3} j(K)^4 \right) \\
& = \frac{1}{2} \frac{2k_B T_m}{V K^2} \frac{1}{K^2} + O \left(\frac{1}{K^4} \right) \\
& = \frac{1}{2} \frac{2k_B T_m}{V K^2} \frac{1}{K^2} + O \left(\frac{1}{K^4} \right) \quad (B16)
\end{aligned}$$

for short range correlations where the K^{-2} term dominates the K^{-4} term, and this finally results in

$$\begin{aligned}
D_j(K)^E & = \frac{\frac{1}{2} \frac{2k_B T_m}{V K^2} \frac{1}{K^2}}{\frac{2k_B T_m}{V K^2} \frac{1}{4k_B T_m} \frac{V c c^2 + 3}{3^2 3} \frac{3}{4} \frac{2k_B T_m a^3}{V K^2} \frac{1}{K^2} + O \left(\frac{1}{K^7} \right)} \\
& = \frac{\frac{1}{2} \frac{V K^2}{2k_B T_m a^3}}{\frac{V K^2}{2k_B T_m} \frac{V^2 c c^2 + 3}{16k_B T_m} + O \left(\frac{1}{K^2} \right)} \\
& = \frac{k_B T_m}{V} \frac{K^2}{\frac{1}{4} \frac{3k_B T_m}{2^2 3} c c^2 + 3 + O \left(\frac{1}{K^2} \right)} : \quad (B17)
\end{aligned}$$

Let

$$M^*(K) = \frac{K^2}{2K^4 - \frac{1}{4} \frac{3k_B T_m}{2^2 3} c c^2 + 3 + O \left(\frac{1}{K^2} \right)}; \quad (B18)$$

$$M(K) = \frac{K^2}{2K^4 - \frac{1}{4} \frac{3k_B T_m}{2^2 3} c c^2 + 3} : \quad (B19)$$

where K is a complex variable in general. $M^*(K)$ has six poles. Three of these poles lie above the real axis, and the other three conjugate poles lie below the real axis. $M(K)$, which is an approximation of $M^*(K)$, has four poles. Among the four, there are two poles on the real K axis corresponding to the four poles of $M^*(K)$ that lie near the real axis. The two real poles of $M(K)$ contribute to a sinusoidal wave. The Green function corresponding to this

non-Gaussian fluctuation is then

$$\begin{aligned}
 G(r) &= \frac{V}{(2\pi)^3} \int d^3K \int_0^Z j(K)^2 e^{iK \cdot r} \\
 &= \frac{V}{(2\pi)^3} \int_0^Z K^2 dK \int_0^Z e^{iK r \cos \theta} \sin \theta d\theta \int_0^Z j(K)^2 \\
 &= \frac{k_B T_m}{4\pi^2 r} \int_0^Z M''(K) K \sin K r dK \\
 &= \frac{k_B T_m}{8\pi^2 r} \frac{\partial}{\partial r} \int_0^Z M''(K) \cos K r dK \\
 &= \frac{k_B T_m}{4\pi^2 r} \frac{\partial}{\partial r} \int_0^Z \text{Im} K > 0 \text{res}(M''(K) e^{iK r}; K) \\
 &= \frac{k_B T_m}{4\pi^2 r} \frac{\partial}{\partial r} \int_0^Z \text{Im} K > 0 \text{res}(M''(K) e^{iK r}; K) + \int_0^Z \text{Im} K = 0 \text{res}(M''(K) e^{iK r}; K) \\
 &= \frac{k_B T_m}{8\pi^2 r} e^{K_0 r} + \cos K_0 r : \tag{B 20}
 \end{aligned}$$

Here,

$$K_0^4 = \frac{1}{4} = \frac{1}{4} \frac{3k_B T_m}{2\pi^2} c^2 + 3 \tag{B 21}$$

which means

$$\begin{aligned}
 &= \frac{4\pi^2 2\pi^2 3=2}{3k_B T_m c^2 (c^2 + 3) a^3} \\
 &= \frac{2\pi^2 2\pi^2}{3k_B T_m a^3} \tag{B 22}
 \end{aligned}$$

where the NNN atom distance a is restored. Therefore,

$$r_{\min} = \frac{2\pi^2 2\pi^2}{3k_B T_m a^3} \tag{B 23}$$

gives an estimation of the minimal diameter of unstable clusters in the solid when $T = T_m$.

My Present Address: Department of Chemistry and Chemical Biology, Harvard University, Cambridge, MA 02138, USA.

To whom correspondence should be addressed.
Email: xfjin@fudan.ac.cn

- ¹ R.W. Cahn, Nature (London) 273, 491 (1978); 273, 668 (1986)
- ² J.G. Dash, Rev. Mod. Phys. 71, 1737 (1999)
- ³ F.A. Lindemann, Phys. Zeit. 11, 609 (1910)
- ⁴ J.J. Gilvarry, Phys. Rev. 102, 308 (1956)
- ⁵ M. Bomm, J. Chem. Phys. 7, 591 (1939)
- ⁶ Z.H. Jin, P. Gumbach, K. Lu and E.M. Ma, Phys. Rev. Lett. 87, 055703 (2001)
- ⁷ J.L. Tallon, Phil. Mag. A 39, 151 (1978)
- ⁸ G. Grimvall and S. Sjodin, Physica Scripta, 10, 340 (1974)
- ⁹ A. Tryanov and E. Tosatti, Phys. Rev. B, 38, 6961 (1988); R. Ohnesorge, H. Lowen and H. Wagner, Phys. Rev. E, 50, 4801 (1994); J.Q. Broughton and G.H. Gilmer, J. Chem. Phys. 79, 5095 (1983); 79, 5105 (1983)
- ¹⁰ F.H. Stillinger and T.A. Weber, J. Chem. Phys. 81, 5095 (1984)
- ¹¹ J. Cardy, J. Phys. A: Math. Gen. 29, 1897 (1996)
- ¹² A.V. Guranato, Phys. Rev. Lett. 68, 974 (1992)

- ¹³ M.I. Baskes, Phys. Rev. Lett. 83, 2592 (1999)
- ¹⁴ V. Halpern, J. Phys. Condens. Matter 12, 4303 (2000)
- ¹⁵ N. Sandberg, B. Magyari-Kope, and T.R. Mattsson, Phys. Rev. Lett. 89, 065901 (2002)
- ¹⁶ K. Nordlund and R.S. Averback, Phys. Rev. Lett. 80, 4201 (1998)
- ¹⁷ A. Bongiorno, L. Colombo, F. Cargnoni, C. Gatti and M. Rosati, Europhys. Lett., 50, 608 (2000)
- ¹⁸ S. Binner, J.P. Goss and R. Jones, P.R. Biddon, S. Oberg, Proceedings of ENDEASD (Stockholm 2000)
- ¹⁹ J.I. Landman and C.G. Morgan, J.T. Schick, P. Papoulias and A. Kummar, Phys. Rev. B 55, 15581 (1997)
- ²⁰ K.W. Ingle, R.C. Perrin and H.R. Schober, J. Phys. F: Metal Phys, 11, 1161 (1981)
- ²¹ L. Salter, Proc. Roy. Soc. (London) A 233, 418 (1956); L. Dobrzynski and J. Friedel, Surf. Science 12, 649 (1968); G. Allan and M. Lannoo, in Defects and Radiation Effects in Semiconductors (ed. R.R. Hasiguti), The Institute of

- Physics (Bristol and London), 1980
- ²¹ R. K. Pathria, *Statistical Mechanics*, 2nd ed., Elsevier (Singapore) Pte Ltd, 2001
 - ²² Kerson Huang, *Introduction to Statistical Physics*, Taylor & Francis, 2001
 - ²³ C. N. Yang and T. D. Lee, *Phys. Rev.* **87**, 404 (1957)
T. D. Lee and C. N. Yang, *Phys. Rev.* **87**, 410 (1957).
 - ²⁴ L. D. Landau and E. M. Lifshitz, *Statistical Mechanics*, Part I (Butterworth-Heinemann, 1999)
 - ²⁵ A. F. Barabanov and V. M. Berezovski, *Zh. Eksp. Teor. Fiz.* **106**, 1156 (1994); H. Rosner, R. Hayn and J. Schulenburg, *Phys. Rev. B* **57**, 13660 (1998); J. Richter, A. Voigt, J. Schulenburg, N. B. Ivanov and R. Hayn, *J. Magn. Magn. Mat.* **177-181**, 737 (1998)
 - ²⁶ N. Goldenfeld, *Lectures on Phase Transitions and the Renormalization Group* (Addison Wesley, 1992)
 - ²⁷ V. L. Ginzburg, *Sov. Phys. Solid State* **2**, 1824 (1960)
 - ²⁸ J. D. Jackson, *Classical Electrodynamics*, 3rd ed., Wiley Text Books, 1998
 - ²⁹ P. Bak, *Phys. Rev. Lett.* **54**, 1517 (1985)